DMD Fast Forward. Published on December 18, 2020 as DOI: 10.1124/dmd.120.000281
This article has not been copyedited and formatted. The final version may differ from this version.

Evaluation of tissue stem cell derived human intestinal organoids, a physiologically relevant model to evaluate cytochrome P450 induction in gut

David M. Stresser[1]*, Jun Sun[1], Sarah S. Wilson[2]

Affiliations

AbbVie, Inc, 1 North Waukegan Road, North Chicago, IL 60064, USA (D.M.S, J.S.)

AbbVie Cambridge Research Center, 200 Sidney Street, Cambridge, MA 02139, USA (S.S.W)

Running title: Intestinal organoid induction model

*Corresponding author:

David M. Stresser

Drug Metabolism and Pharmacokinetics

AbbVie

1 North Waukegan Road

North Chicago, IL 60064 USA

Tel: 847-935-4327; Fax: 847-937-8330

E-mail: David.Stresser@abbvie.com

Number of text pages: 15

Number of tables: 0

Number of figures: 9

Number of references: 52

Number of words, abstract: 245

Number of words, introduction: 909

Number of words, discussion: 1560

List of Abbreviations

ADME, absorption, distribution, metabolism, excretion; BCRP, breast cancer resistance protein; CAR, constitutive androstane receptor; Ct value, cycle threshold value; CYP or P450, cytochrome P450; Pgp, P-glycoprotein; MDR1, multidrug resistance transporter 1; CITCO, 6-(4-chlorophenyl)imidazo[2,1-b][1,3]thiazole-5-carbaldehyde O-(3,4-dichlorobenzyl)oxime; DMSO, dimethyl sulfoxide; iPS, induced pluripotent stem; PCR, polymerase chain reaction; PXR, pregnane X receptor; UGT, UDP-glucuronosyl

DMD Fast Forward. Published on December 18, 2020 as DOI: 10.1124/dmd.120.000281
This article has not been copyedited and formatted. The final version may differ from this version.

transferase; WRN conditioned media, Wnt3a R-spondin Noggin conditioned media; EC_{50}, concentration at which there is a 50% maximal induction; Emax, maximal fold-induction.

Abstract

Induction of cytochrome P450 (CYP) can cause drug-drug interactions and efficacy failure. Induction risk in liver and gut is typically inferred from experiments with plated hepatocytes. Organoids are physiologically relevant, multi-cellular structures originating from stem cells. Intestinal stem-cell derived organoids retain traits of normal gut physiology, such as an epithelial barrier and cellular diversity. Matched human enteroid and colonoid lines, generated from ileal and colon biopsies from two donors, were cultured in extracellular matrix for three days, followed by a single 48h treatment with rifampin, omeprazole, CITCO and phenytoin at concentrations that induce target genes in hepatocytes. Following treatment, mRNA was analyzed for induction of target genes. Rifampin induced CYP3A4; estimated EC_{50} and E_{max} were 3.75 µM and 8.96-fold, respectively for ileal organoids, and 1.40 µM and 11.3-fold, respectively, for colon organoids. Ileal, but not colon organoids exhibited nifedipine oxidase activity, which was induced by rifampin up to 14-fold. The test compounds did not increase mRNA expression of CYP1A2, CYP2B6, MDR1 (Pgp), BCRP and UGT1A1 in ileal organoids. Whereas omeprazole induced CYP3A4 (up to 5.3-fold, geomean, n = 4 experiments), CAR activators phenytoin and CITCO did not. Omeprazole failed to induce CYP1A2 mRNA, but induced CYP1A1 mRNA (up to 7.7-fold and 15-fold in ileal and colon organoids, respectively, n = 4 experiments). Despite relatively high intra- and interexperimental variability, data suggest that the model yields induction responses which are distinct from hepatocytes and holds promise to enable evaluation of CYP1A1 and CYP3A4 induction in gut.

DMD Fast Forward. Published on December 18, 2020 as DOI: 10.1124/dmd.120.000281
This article has not been copyedited and formatted. The final version may differ from this version.

Significance Statement

An adult intestinal stem-cell derived organoid model to test cytochrome P450 induction in gut was evaluated. Testing several prototypical inducers for mRNA induction of P450 isoforms, UGT1A1, Pgp and BCRP with both human colon and ileal organoids resulted in a range of responses, often distinct from those found in hepatocytes, indicating the potential for further development of this model as a physiologically relevant gut induction test system.

DMD Fast Forward. Published on December 18, 2020 as DOI: 10.1124/dmd.120.000281
This article has not been copyedited and formatted. The final version may differ from this version.

Introduction

Induction of cytochrome P450 enzymes by a drug candidate may lead to unwanted increases in the rate of metabolism and elimination of itself or co-medications. Although induction may occur in multiple tissues, liver and gut are tissues where induction is considered quantitatively meaningful in affecting pharmacokinetics. Preclinical or in vitro methods to evaluate induction in gut are generally lacking. Therefore, the prediction of gut induction response is typically inferred from studies conducted in plated human hepatocytes. This practice is typically applied to CYP3A4 inducers only, as the enzyme is expressed and inducible in both liver and gut. However, some compounds, such as efavirenz and carbamazepine have been shown to induce CYP3A in liver, but not in gut (Mouly et al, 2002; Meyer et al, 2012; Giessmann et al, 2004) indicating a hepatocyte model for induction may not always be appropriate. One explanation for these observations is that enterocytes respond differently to inducing agents compared to hepatocytes. Indeed, the identity and relative abundance of enzymes and transporters expressed in gut are distinct from that in liver suggesting gene-expression and induction regulatory mechanisms may differ between the two tissues. For example, expression of CYP2C8, CYP1A2, CYP2B6, while significant in liver, is generally reported absent in gut (Paine et al, 2006; Drozdzik et al, 2018). Conversely, expression of CYP1A1 and UGT1A10 are observed in gut, but not liver (Paine et al, 2006; Oda et al 2017). Since the fraction of drug absorbed and metabolized in gut wall is a critical component of overall oral bioavailability, evaluating the inducibility of drug metabolizing enzymes and transporters in models derived from intestine, rather than from liver, would be desirable.

Drug oral bioavailability (F) may be described as the fraction of oral drug escaping gut metabolism and transporter-mediated secretion (F_g) multiplied by the fraction absorbed (F_a) and the fraction metabolized in liver or excreted into bile (F_h). In a literature survey of > 300 compounds with abundant human pharmacokinetic data, approximately 30% exhibited F_g of 0.8 or less (Varma et al, 2010), demonstrating the important role of gut metabolism in estimating F. Many compounds exhibiting a substantial F_g component are metabolically unstable and are substrates of CYP3A4 and efflux

DMD Fast Forward. Published on December 18, 2020 as DOI: 10.1124/dmd.120.000281
This article has not been copyedited and formatted. The final version may differ from this version.

transporters (Zhang and Benet, 2001). Induction of CYP3A4 and/or efflux transporters in gut could affect F_g and mediate drug-drug interactions (Galetin et al, 2010; Alqahtani et al, 2018). Attempts to evaluate P450 induction in gut using colon carcinoma-derived cell lines have met with limited success and are generally considered of questionable relevance. The caco-2 cell line is widely deployed to study intestinal permeability and transport, but is not suitable for evaluating CYP3A4 induction and regulation because it lacks PXR (Thummel et al, 2001; Schmiedlin-Ren et al, 2001; Hartley et al, 2006; Brück et al, 2017). Another colon carcinoma cell line, LS-180, is responsive to PXR-mediated inducers but may exhibit atypical gene expression while lacking the advantages of primary cells (Schuetz et al, 1996; Gupta et al, 2008; Zheng et al, 2012). Recently, cryopreserved human intestinal mucosal epithelium, consisting of multicellular fragments from villi of multiple donors have become commercially available (Li et al, 2018). Incubation of these fragments with rifampin or 1, 25-dihydroxyvitamin D3 resulted in up to a 3-fold induction of CYP3A4 mRNA, thereby offering a model using human tissue-derived material. A potential limitation of this model is the dynamic range of the induction response and longevity of the cultures upon thawing, which is apparently 3-fold and up to 24 hours, respectively.

Advanced microphysiological systems and three-dimensional tissue culture models continue to gain in popularity. By incorporating attributes such as multiplicity of cell types, three-dimensional architecture, flow and mechanical motion, in vivo-like function is purported to be superior to conventional two-dimensional cell culture models (Madden et al, 2018; Fowler et al, 2020). Organoids are tissue-mimetic, microphysiological, three-dimensional structures, experimentally derived from stem cells (Fatehullah et al, 2016). Human intestinal organoids retain several traits of normal gut physiology, mirroring the microenvironment and function of the epithelial barrier and cell diversity of the gastrointestinal tract - stem cells readily divide and give rise to Paneth and goblet cells, as well as enterocytes. These models have recently gained interest from drug metabolism scientists evaluating induction and other ADME parameters. Onozato et al (2018) used an iPS cell-derived intestinal organoid model to evaluate induction of CYP3A4 and other enzymes. In this study, following the 31-day culture

DMD Fast Forward. Published on December 18, 2020 as DOI: 10.1124/dmd.120.000281
This article has not been copyedited and formatted. The final version may differ from this version.

and differentiation period, a single 3-day treatment of 40 μM rifampin was given, and induced CYP3A4 mRNA 2-fold. Authors concluded there was a need to develop an improved differentiation protocol to increase induction response levels. More recently, adult stem-cell derived duodenal organoids, isolated into fragments and seeded to form monolayers on polydimethylsiloxane chips were used to demonstrate a 5.3-fold induction of CYP3A4 mRNA by 20 μM rifampin treatment (Kasendra et al, 2020).

Human ileal and colon organoid cultures have been established as pharmacology models in our laboratory, using adult tissue-resident stem cells based on methods developed previously (VanDussen et al, 2015). In this investigation, the effect of several prototypical inducers on the mRNA expression of CYP3A4 and other P450 isoforms, UGT1A1, Pgp and BCRP with both human colon and ileal organoids were investigated. We demonstrate the model can exhibit significant induction responses (> 10-fold, depending on inducer and target) that are drug concentration dependent. Responses for some compounds were often distinct from those found in hepatocytes and indicate the potential for further development of this model as a physiologically relevant gut induction test system.

DMD Fast Forward. Published on December 18, 2020 as DOI: 10.1124/dmd.120.000281
This article has not been copyedited and formatted. The final version may differ from this version.

Materials and Methods

Organoid establishment and culture. Established human ileal and colon organoid lines were obtained from the Stappenbeck and Ciorba labs at the University of Washington in St. Louis (VanDussen et al, 2015; VanDussen et al, 2019). Lines were derived from biopsy samples from donors of unknown sex and the collection and use of human intestinal tissue for spheroid culture was approved by the Institutional Review Board of Washington University School of Medicine and written informed consent was obtained from the donors prior to inclusion in the study. For routine culture, organoids were grown in 15 µl plugs of growth factor-reduced Matrigel (Corning, Corning, NY) in 48 well plates and overlaid with 350 µl growth media containing Wnt3a, Rspondin3 and Noggin. Growth media was comprised of Advanced DMEM/F12 (ThermoFisher Scientific #12634-010), 1x GlutaMAX (ThermoFisher Scientific #35050), 1x Penicillin/Streptomycin (ThermoFisher Scientific #15140) and 20% FBS (Sigma #F2442) to which was added at a 1:1 ratio of conditioned media derived from L-WRN cell line (ATCC#CRL-3276), 10 µM Y-27632 (ROCK inhibitor, Tocris, Minneapolis, MN), and 10 µM SB-431542 (TGF-ßRI inhibitor, Tocris). Organoids were passaged every 3-4 days using mechanical dissociation and trypsin (Millipore Sigma). The production and quality control of L-WRN conditioned media produced from the L-WRN cell line, as well as its utilization to support human ileal and colon organoids culture has been described in detail elsewhere (VanDussen et al, 2019; Miyoshi and Stappenbeck, 2013). For this study, conditioned media collected on each day of days 1-4, filtered using 0.22 micron polyethersulfone filters and frozen was used in growth media for all assays.

Organoid model and induction experiments. To normalize organoid seeding for assays, after trypsinization and manual pipetting for disruption into single cells, organoids were filtered through a 40-micron filter and spun down in growth media. Organoid pellets were then resuspended in 1 mL of the growth media, and a 15 µl aliquot of this sample was removed and then diluted two-fold up to a 1:16 dilution in growth media. 10 µl of this organoid suspension was then added to black-walled clear bottom

DMD Fast Forward. Published on December 18, 2020 as DOI: 10.1124/dmd.120.000281
This article has not been copyedited and formatted. The final version may differ from this version.

96-well plate containing 100 µl *CellTiter-Glo® 3D* (Promega #G9683) + 100 ul of PBS. The plate was protected from light and incubated at RT for 30 min, with shaking for the first 5 min. During incubation, stock solution of colonoids was kept in growth media on ice. For plating, the solution of colonoids in washing media was spun at 5 min, 600 g, ambient temperature, in a 50 mL conical tube as above. Media was aspirated, and pellet resuspended in the appropriate volume of thawed Matrigel, with the dilution dependent on normalization to a pre-selected value based on luminescence readings. The preferred density for plating and corresponding luminescence value was experimentally evaluated and is dependent on the machine used to read luminescence. Once solidified, Matrigel plugs were overlaid with growth media as described above but with addition of 100 nM dexamethasone. Organoids were allowed to grow and expand in Matrigel for 3 days, after which media was aspirated and replaced with Advanced DMEM/F12 containing L-glutamine, Penicillin/Streptomycin, 50 ng/mL recombinant human EGF (Thermo Fisher Scientific), 100 nM dexamethasone and test inducer compounds at indicated concentrations or DMSO vehicle control.

Enzyme activity. CYP3A4 enzyme activity was determined by measuring oxidation of nifedipine after 48h treatment of organoids with rifampin or solvent vehicle control. Media was aspirated from wells, and organoid plugs were washed once with PBS before being overlaid with 300 µL Advanced DMEM/F12 containing L-glutamine, penicillin/streptomycin, 50 ng/mL recombinant human EGF and 5 or 50 µM nifedipine. A time zero sample (150 µL) was removed, and after incubating 60 min or 360 min at 37°C the remaining 150 µl was collected. Dehydro-nifedipine was quantified by LC/MS using verapamil as an internal standard.

Viability assessment. To assess organoid survival after inducer treatment, media was aspirated and matrigel plugs were overlaid with 100 µl of Cell-titer GLO 3D and 100 µl of PBS, incubated while shaking for 30 mins at ambient temperature, and then volume transferred to a 96 well clear bottom black well plate for luminescence reading on an Envision 2105 Multimode plate reader.

DMD Fast Forward. Published on December 18, 2020 as DOI: 10.1124/dmd.120.000281
This article has not been copyedited and formatted. The final version may differ from this version.

RNA isolation. Following inducer treatments (and nifedipine incubations, if applicable), matrigel plugs were washed with PBS and resuspended in RNAlater® (Thermo Fisher Scientific) and kept frozen (-80°C) for subsequent RNA isolation. The mRNA from organoids was extracted with MagMax™ – 96 Total RNA isolation kit.

RTPCR. In previous investigations (and shown in Figure 8 for 18S values), we observed consistent recovery of mRNA across well plates. Therefore, after RNA extraction, a fixed volume of total RNA was reverse transcribed into cDNA (SuperScript™ VILO™ cDNA-synthesis kit). RTPCR was performed on ViiA7 or QuantStudio real-time PCR system using TaqMan Assays-on-Demand™ Gene Expression assays to assess expression of target genes and normalized to the housekeeping gene GAPDH or, for NR1I2 (PXR) and NR1I3 (CAR) only, 18S ribosomal RNA. The following assay IDs for the TaqMan Gene Expression assays were used: CYP3A4, Hs00604506_m1; CYP1A1, Hs02382618_s1; CYP1A2, Hs00167927_m1; CYP2B6, Hs03044634_m1; UGT1A1, Hs02511055_s1; P-gp, Hs01394345_g1; BCRP, Hs01053790_m1; GAPDH, Hs02786624_g1; NR1I2, Hs_00901571; NR1I3, Hs00901571_m1, 18S ribosomal RNA, Hs99999901_s1).

RNA-sequence expression analysis. Tissue expression data are from the Genotype-Tissue Expression (GTEx) Portal (https://gtexportal.org/home/) accessed on 14 November, 2020 and expressed as transcripts per million.

Statistical Analysis. For non-parametric data, statistical significance between groups was conducted using Kruskal-Wallis non-parametric test within Prism software, followed by Dunn's multiple comparisons if statistical significance ($\alpha = 0.05$) was indicated. Unpaired t-tests were used to compare the effect of rifampin on nifedipine oxidase activities in ileal organoids.

Curve-fitting. The EC_{50} and E_{max} values were generated by non-linear curve-fitting using a 4-parameter model, Y=Bottom + (X^Hillslope)*(Top-Bottom)/(X^HillSlope + EC50^HillSlope) with the bottom constrained to 1.

DMD Fast Forward. Published on December 18, 2020 as DOI: 10.1124/dmd.120.000281
This article has not been copyedited and formatted. The final version may differ from this version.

DMD Fast Forward. Published on December 18, 2020 as DOI: 10.1124/dmd.120.000281
This article has not been copyedited and formatted. The final version may differ from this version.

Results

Establishing the model. When intestinal organoids are grown in Wnt3a-containing media, such as the Wnt3a-Rspondin-Noggin(WRN)-conditioned media used in this study, they are stem-cell enriched and characterized by their cystic appearance with thin cell layers and large lumens (VanDussen et al, 2015). Upon removal of Wnt from the culture media, stem cells rapidly differentiate into epithelial cell types including Goblet cells, enteroendocrine cells, and enterocytes (Sato et al, 2011). To enable the establishment of a model to look at induction of drug-metabolizing enzymes in human enterocytes, organoids were grown for 3 days in WRN conditioned media + dexamethasone to allow for stem cell expansion. This was followed by 2 days of growth in media (Advanced DMEM/F12 containing L-glutamine, Penicillin/Streptomycin/dexamethasone) containing EGF as the only growth factor (media + EGF in figures) in the presence or absence of the inducers. It should be noted that the choice to include dexamethasone in the media was based on previous findings that a glucocorticoid agonist is required for robust manifestation of CYP3A4 induction in hepatocytes (Pascussi et al, 2000). Whether it is required for CYP3A4 induction in this test system is not yet known. Media supplemented with EGF growth factor was chosen as we have shown this composition enriches for the differentiated cells which would be present in the small intestinal villus and the top of a colonic crypt over cells which are present in the base of a crypt such as intestinal stem cells. Specifically, growth in media + EGF results in an increase in the goblet cell marker Mucin2 and the enterocyte marker sucrose isomaltose in organoids compared to organoids grown in WRN conditioned media, which is rich in growth factors as it contains both FBS as well as conditioned media derived Wnt3a, Rspondin, and Noggin a. This is accompanied by a loss of expression of the stem cell marker LGR5 and the proliferation marker Ki67 in organoids grown in media + EGF compared to those grown in WRN conditioned media (Supplemental Figure).

The question may arise about the relevance of an enclosed test system where the organoid interior space corresponds to the lumen of the intestine. For example, the interior may accumulate shed cellular debris, otherwise eliminated by lumenal content flow in normal gut physiology. Indeed, in vivo the

DMD Fast Forward. Published on December 18, 2020 as DOI: 10.1124/dmd.120.000281
This article has not been copyedited and formatted. The final version may differ from this version.

estimation is that it takes 4-5 days for a stem cell to differentiate to an enterocyte and move up the crypt-villus axis before being shed into the intestinal lumen (Clevers and Bevins, 2013). In organoid culture, accumulation of cellular debris in the organoid lumen is observed after long-term culture of 7-10 days (Sato et al, 2009). A consideration for the timing of our assay setup is the health of the organoids which includes a lack of cellular debris in the lumen. As our assay runs for only 5 days, we do not see significant accumulation of shed enterocytes within the lumen of the organoids and therefore do not anticipate significant impact on the estimation of induction.

Cytochrome P450, UGT and transporter inducibility in ileal and colon organoids by rifampin. In order to determine the utility of this model for understanding the expression of drug-metabolizing enzymes in the gut, a time course experiment with 100 µM rifampin as the inducer was carried out for 0, 4, 24, 48 and 72 hours in ileal organoids (Figure 1). These data showed robust induction response generally greater than 4-fold, from 24 to 72h. Based on these data, subsequent experiments for all inducers were carried out with a single 48h exposure time. The effect of increasing concentrations of rifampin on CYP3A4 induction in ileal and colon organoids is shown in Figure 2, with each circle representing the response from organoids pooled from two matrigel plugs. For both ileal and colon organoids, induction by rifampin was marked by statistically significant concentration dependence but also by marked variability (Figure 2, panels A and C) across multiple experiments. The estimated EC_{50} and E_{max} for CYP3A4 were 3.75 µM and 8.96, respectively with a Hill slope of 0.44 for ileal organoids. For colon organoids, estimated EC_{50} and E_{max} were 1.40 µM and 11.3, respectively, with a Hill slope of 0.97. Grey and blue circles represent data from two different donors and these data indicated no marked donor-dependent differences in response. Next, the effect of rifampin on other selected transcripts (CYP1A1, CYP2B6, UGT1A1, Pgp, BCRP) is shown in comparison to CYP3A4 generated within the same experiment (except CYP1A1, which was an independent experiment) in ileal and colon organoids (Figure 2, panels B and D). Unlike with CYP3A4, rifampin caused no increase in other transcripts.

DMD Fast Forward. Published on December 18, 2020 as DOI: 10.1124/dmd.120.000281
This article has not been copyedited and formatted. The final version may differ from this version.

Effect of various inducers on CYP3A4, CYP1A1 and CYP2B6 induction in ileal and colon organoids. To further understand induction responses in the organoid model, the effect of other prototypical inducers, such as CAR activators phenytoin and CITCO and the AhR activator omeprazole on induction of CYP3A4 mRNA was performed. As shown in Figure 3 (panel A, ileal organoids; panel B, colon organoids), responses between tissues were remarkably similar despite relatively high variability when an induction response was indicated. The effect of rifampin, phenytoin and omeprazole on CYP1A1 mRNA induction is shown in Figure 4. While omeprazole treatment resulted in a concentration dependent and variable increase in CYP1A1 mRNA in both ileal (geomean of 7.7-fold, 95% CI 1.05-8.44, at 100 µM omeprazole) and colon organoids (15.2-fold, 95% CI 3.04-76.3, at 100 µM omeprazole), other test compounds showed no evidence of induction. Figure 5 shows the effect of rifampin, phenytoin, CITCO and omeprazole on CYP2B6 mRNA. In general, these compounds caused no induction of CYP2B6, with the exception of omeprazole which appeared to induce CYP2B6 in a concentration-dependent manner in both ileal and colon organoids. One data point among the replicates for both rifampin (100 µM) and CITCO indicated CYP2B6 induction, but these appeared to be spurious. Several attempts were made with various inducers to induce CYP1A2 in ileal and colon organoids, but this transcript was consistently found to be undetectable (e.g. Ct values > 35).

CYP3A4 enzyme activity can be detected in intestinal organoids. To determine if the observed mRNA increases corresponded to functional protein activity, we measured the CYP3A4 enzyme activity in rifampin treated ileal organoids. Figure 6, panel A shows the accumulation of dehydro-nifedipine in incubations of rifampin-treated ileal organoids with 5 or 50 µM nifedipine, a CYP3A4 probe substrate, after either 1- or 6-hour incubations in comparison to organoids treated with DMSO solvent vehicle only. While enzyme activity was not detected after 1h incubations, 6h incubations demonstrated CYP3A4-catalyzed dehydro nifedipine metabolite formation. Using 5 and 50 µM nifedipine as substrate rifampin treatment induced dehydro nifedipine metabolite formation by 3.4- and 14.3-fold, respectively. It should be noted that formation of dehydro nifedipine may not have been linear with incubation time, which may

DMD Fast Forward. Published on December 18, 2020 as DOI: 10.1124/dmd.120.000281
This article has not been copyedited and formatted. The final version may differ from this version.

explain the fold-induction disparity between the 5 and 50 µM nifedipine incubations. Nevertheless, these data demonstrate induction of CYP3A4 transcript (Figure 6, panel B) was accompanied by induction of CYP3A4 enzyme activity.

Cytotoxicity of test compounds. As the lack of transcriptional induction observed after treatment with some inducers might be explained by cytotoxicity, the effect of various treatments on organoid cell viability was measured in each study and is shown in Figure 7. In all cases organoids remained viable across treatments, with the exception of rifampin at 300 µM and omeprazole at 200 µM. Therefore, CYP induction data generated at these high concentrations were excluded from analysis.

PXR and CAR expression in ileal and colon organoids. In order to understand the mechanisms that may underlie the observed induction patterns in our organoid model, we investigated expression of PXR (NR1I2) and CAR (NR1I3) RNA in ileal and colon organoids from donor 1, at various times during the assay and after rifampin treatment (Figure 8). The green squares represent the day 3 expression at the beginning of the assay when the inducers would be added, while the blue triangle represent the expression in control samples on day 5 at the end of the assay, and the purple triangles represent the expression on day 5 after rifampin treatment. In all treatments, based on Ct values, expression of PXR is much higher than CAR in both ileal and colon organoids. PXR had Ct values ranging between 28 and 34, while CAR Ct values were all over 35 and in some cases undetectable, indicating lower levels or absence of expression in the model.

DMD Fast Forward. Published on December 18, 2020 as DOI: 10.1124/dmd.120.000281
This article has not been copyedited and formatted. The final version may differ from this version.

Discussion

Organoids are multicellular micro-structures exhibiting several desirable characteristics of an in vitro gut induction model. First, organoids (in this study) are grown from human tissue biopsies, generating a multi-cell type primary assay, with an expected improvement over immortalized cell culture systems (Sato et al. 2009; VanDussen et al, 2015). Second, organoid lines can be frozen and banked, enabling repeat testing of compounds from the same donor. Third, organoid cultures can be established in multi-well formats, facilitating concentration-response studies necessary to establish potency. Fourth, as demonstrated in this study, organoids can exhibit robust induction of mRNA and/or catalytic activity in response to compound treatment.

In contrast to iPS cell-derived organoids used by Onozato et al (2018), we used organoids derived from biopsy specimens. These two culture methods differ in that biopsy-derived organoid lines require less time to grow and differentiate into organoids (3-5 days versus up to 34 days). In addition, our stem-cell derived organoids are comprised of epithelial cells only, versus iPS cell-derived organoids which contain mesenchymal cell markers (i.e. α-smooth muscle actin) (VanDussen et al 2015; Onozato et al, 2018). Whereas Onozato et al achieved ~ 2-fold CYP3A4 mRNA induction in response to rifampin treatment, we observed 9- to 11-fold induction in our model. Whether use of tissue stem cell derived organoids or another aspect of our protocol, enabled the higher induction response warrants further study.

In evaluating our model, we tested AhR, CAR or PXR activators, with a focus on rifampin as a PXR activator and well-characterized CYP3A4 inducer. Drug concentrations were selected to mimic those that well-induce target CYP enzymes in hepatocyte models and were generally lower (~2 to 10-fold) than intestinal lumen concentrations estimated as dose/250 mL (Zhang et al, 2008). In some cases, initially desired concentrations were adjusted lower to ensure adequate solubility (phenytoin) or avoid apparent cytotoxicity (omeprazole, rifampin). The concentration of CITCO was chosen to be selective for CAR, while avoiding significant PXR activation (Maglich et al, 2003). With rifampin, EC_{50} values in

DMD Fast Forward. Published on December 18, 2020 as DOI: 10.1124/dmd.120.000281
This article has not been copyedited and formatted. The final version may differ from this version.

ileal and colon organoids were 3.75 and 1.4 µM, respectively. These compare to typical findings in hepatocytes, showing rifampin EC_{50} values generally ranging between 0.1 and 1 µM (https://didb.druginteractionsolutions.org/, accessed 17 November, 2020). Complicating the estimation of kinetic parameters was the relatively high inter- and intra-experimental variability observed. Data variability did not seem to be donor-dependent, as testing in a second donor gave similar results (indicated as blue symbols in plots containing grey symbols) and may be the result of the more complex and cellularly diverse organoid system. Another consideration in interpreting differences in kinetic parameters is that intracellular exposure may vary compared to hepatocytes perhaps due to organoid architecture (inability to directly access to the apical side interior) or relative expression of uptake and efflux transporters.

We also evaluated effect of rifampin on other transcripts. Data in Figure 2 shows that while CYP3A4 was induced in a concentration dependent manner, CYP1A1, CYP2B6, UGT1A1, Pgp or BCRP exhibited no induction. Absent CYP1A1 induction might be expected since rifampin is not known to induce this enzyme. Lack of UGT1A1 induction was also unsurprising as rifampin did not increase UGT1A1-catalyzed estradiol 3-glucuronidation in hepatocytes (Soars et al, 2004). However, one might expect induction of CYP2B6, since rifampin readily induces CYP2B6 in hepatocytes (discussed further below). No induction of Pgp mRNA was observed contrasting findings that mRNA was induced in duodenal biopsies in individuals given rifampin (Brueck et al, 2019; Greiner et al, 1999; Larsen et al, 2007). In the aforementioned biopsy studies, the fold induction was rather modest (~ 1.3 to 3.5-fold). Absence of Pgp induction is possibly attributable to differences in the relative percentage of enterocytes (i.e., the cell-type believed responsive to inducing agents) in organoids compared to biopsy tissue. Absence of rifampin induction of BCRP in organoids agrees with previous reports in intestinal biopsies (Brueck et al, 2019). It should be noted that the percentage of biopsy mass composed of enterocytes was not reported in those studies suggesting the fold induction by rifampin may be underestimated.

DMD Fast Forward. Published on December 18, 2020 as DOI: 10.1124/dmd.120.000281
This article has not been copyedited and formatted. The final version may differ from this version.

The effect of compounds that predominantly activate CAR (phenytoin or CITCO) or AhR (omeprazole) on CYP3A4 expression was examined (Figure 2). Phenytoin appeared to show relatively weak, concentration dependent induction whereas 0.1 μM CITCO gave no effect. Since both compounds readily induce CYP3A4 in hepatocytes, which highly express CAR, the findings suggested the possibility that CAR mechanisms are absent in organoids. By qPCR, we found CAR levels were about 20-fold lower than PXR in untreated organoids. Subsequent inspection of an RNA-sequencing database in tissues from > 180 cadavers revealed CAR expression is very low in transverse colon and terminal ileum tissue, compared to PXR expression, whereas CAR expression is comparable to PXR in liver (Figure 9). These data are also in agreement with Brueck et al (2019) showing much lower CAR expression in duodenal biopsies. This may in part explain findings that efavirenz and carbamazepine, two CAR preferential activators (Faucette et al, 2007), exhibit induction in liver, but not intestine (Giessmann et al, 2004; Mouly et al, 2002; Meyer et al, 2012). Together, these data suggest compounds inducing CYP3A4 by a CAR-mediated mechanism may not induce CYP3A4 in gut. This has implications for drug development. For example, some compounds could be spared from auto-induction of CYP3A4 clearance in gut or be less prone to induce clearance of co-medications that undergo significant CYP3A4-mediated gut metabolism. Omeprazole induced CYP3A4 (up to 5.3-fold, geomean, n = 4 experiments), which is in line with previous reports of omeprazole as a PXR activator and CYP3A4 inducer (Novotna and Dvorak, 2014) in human hepatocytes.

We also examined CYP1A1 and CYP1A2 induction response by activators and non-activators of AhR. In both ileal and colon organoids, we found CYP1A1 mRNA was highly induced by omeprazole. Consistent with this observation, CYP1A1 protein is detected in meaningful quantities in human small intestinal microsomes and is known to be inducible in this tissue (Fontana et al, 1999; Paine et al, 2006; Zhang et al, 1999). As anticipated, rifampin and phenytoin failed to induce CYP1A1 in either ileal or colon organoids. Omeprazole did not induce CYP1A2 mRNA in organoids nor was the transcript detected, agreeing with reports showing CYP1A2 transcripts or protein undetectable in gut (Thelen and

DMD Fast Forward. Published on December 18, 2020 as DOI: 10.1124/dmd.120.000281
This article has not been copyedited and formatted. The final version may differ from this version.

Dressman, 2009; Paine et al, 2006). We did not detect induction of CYP2B6 by rifampin, phenytoin and CITCO, respectively, in line with reports that CYP2B6 is not expressed in gut mucosa (Paine et al, 2006; Zhang et al, 1999). Interestingly, the CYP2B6 transcript was readily detectable, with Ct values ranging from ~25 to ~ 29 in ileal and colon organoids across the various treatments. This suggests that absence of CYP2B6 protein expression in mucosa may be related to unavailability of cellular systems permitting CYP2B6 translation.

While we evaluated our model with activators of AhR, CAR and PXR, it should be noted that lesser known or atypical pathways that regulate P450 and transporter expression may be present in this tissue, and may exhibit differing relative importance compared liver (Gerbal-Chaloin et al, 2014; Dixit et al, 2005; Müller et al, 2017; Zheng et al, 2012). We did not examine inducibility originating from the various cell types within the organoids. However, as enterocytes are present in the ileal organoids, and enterocytes exhibit relatively high CYP3A4 expression (Zhang et al, 1999; McKinnon et al, 1995; Glaeser et al, 2005), it can be expected that the induction response we measured originated primarily from enterocytes. Similarly, one might expect the same for the colonocyte-like cells in colon organoids. Within the small intestine, the upper portion (jejunum, duodenum) typically exhibits highest concentration of P450 (Zhang et al, 1999), whereas the distal portion (ileum) exhibits higher Pgp expression (Mouly and Paine, 2003). Colon epithelium is not considered a significant contributor to drug metabolism; absorbing surface area is very low - about 0.2% that of the combined surface area of ileum and duodenum (Kararli, 1995) and P450 and other drug metabolizing activities are generally low or undetectable (van de Kerkhof et al, 2008; Peters et al, 1991). Therefore, while the response to inducers in colon organoids in our study were strikingly similar to ileal organoids, both qualitative and quantitatively (e.g., figures 2-5), studies in jejunal and duodenal organoids might be needed to fully predict induction responses in the gastro-intestinal tract.

In sum, we have characterized selected CYP and transporter induction properties of a novel and physiologically relevant gut model. Data demonstrate that organoids, derived from human adult ileal and

colonic stem cells, are a potentially promising test system to evaluate CYP induction. Organoids appear to recapitulate expected intestinal induction responses such as induction of CYP3A4, but not CYP1A2 or CYP2B6. Other notable findings are absence of efflux transporter mRNA induction. CAR mRNA is expressed at levels much lower than PXR in organoids and intestinal tissue, in contrast to liver. Coupled with absence of CYP3A4 induction by CAR activators in this model, our data suggests genes regulated by CAR appears to be non-inducible, and may explain, at least in part, compartmental CYP3A4 induction by some compounds that are predominantly CAR activators. This indicates that the model could be used to de-risk drug candidates identified as CAR-mediated inducers. Limitations to this organoid model include the relative lack of commercial accessibility and relatively high intra-experimental data variability. Future efforts should be aimed at improving assay variability and develop methods to scale data to in vivo response, possibly enabling application to PBPK modeling.

Acknowledgements

Authors would like to thank Sudiksha Chaulagain for experimental support, Hardikkumar Patel for nifedipine oxidase assay bioanalytical support, Kelly Desino for management support, Edda Fiebiger for scientific discussion and Julius Enoru for critical review and comments on the manuscript. All contributors are employees of AbbVie.

Authorship Contributions

Participated in research design: Sun, Wilson, Stresser

Conducted experiments: Sun, Wilson

Contributed new reagents or analytic tools: N/A

Performed data analysis: Sun, Wilson, Stresser

Wrote or contributed to the writing of the manuscript: Sun, Wilson, Stresser

References

Alqahtani S, Bukhari I, Albassam A, Alenazi M (2018) An update on the potential role of intestinal first-pass metabolism for the prediction of drug–drug interactions: the role of PBPK modeling, Expert Opinion on Drug Metabolism & Toxicology, 14:6, 625-634.

Brück S, Strohmeiera J, Buscha D, Drozdzikb M, and Oswald S (2017) Caco-2 cells – expression, regulation and function of drug transporters compared with human jejunal tissue. Biopharm. Drug Dispos. 38: 115–126.

Brueck S, Bruckmueller H, Wegner D, Busch D, Martin P, Oswald S, Cascorbi I, and Siegmund W (2019) Transcriptional and Post-Transcriptional Regulation of Duodenal P-Glycoprotein and MRP2 in Healthy Human Subjects after Chronic Treatment with Rifampin and Carbamazepine. Mol. Pharmaceut. 16, 3823-3830.

Clevers HC and Bevins CL. (2013) Paneth cells: maestros of the small intestinal crypts. Rev Physiol. 75:289-311.

Dixit SG, Tirona RG, Kim RB. Beyond CAR and PXR (2005) Curr Drug Metab. 6:385-97.

Drozdzik M, Busch D, Lapczuk J, Müller J, Ostrowski M, Kurzawski M, and Oswald S (2018) Protein abundance of clinically relevant drug-metabolizing enzymes in the human liver and intestine: a comparative analysis in paired tissue specimens. Clin Pharmacol Ther 104:515-524.

Fatehullah A, Tan S. Barker N (2016) Organoids as an in vitro model of human development and disease. Nat Cell Biol 18: 246–254.

Faucette SR, Zhang TC, Moore R, Sueyoshi T, Omiecinski CJ, LeCluyse EL, Negishi M, and Wang H (2007) Relative activation of human pregnane X receptor versus constitutive androstane receptor defines distinct classes of CYP2B6 and CYP3A4 inducers. J Pharmacol Exp Ther 320:72-80.

Fontana RJ, Lown KS, Paine MF, Fortlage L, Santella RM, Felton JS, Knize MG, Greenburg A and Watkins PB (1999) Effects of a chargrilled meat diet on expression of CYP3A, CYP1A and P-glycoprotein levels in healthy volunteers. Gastroenterology 117:89-98.

Fowler S, Chen WLK, Duignan DB, Gupta A, Hariparsad N, Kenny JR, Lai WG, Liras J, Phillips JA and Gan J (2020) Microphysiological systems for ADME-related applications: current status and recommendations for system development and characterization. Lab Chip, 20: 446-467.

Gerbal-Chaloin S, Dumé A-S, Briolotti P, Klieber S, Raulet E, Duret C, Fabre J-M, Ramos J, Maurel P and Daujat-Chavanieu M (2014) The WNT/β-Catenin Pathway Is a Transcriptional Regulator of CYP2E1, CYP1A2, and Aryl Hydrocarbon Receptor Gene Expression in Primary Human Hepatocytes. Molecular Pharmacology. 86 (6): 624-634.

Galetin A, Gertz M, Houston JB (2010). Contribution of intestinal cytochrome P450-mediated metabolism to drug-drug inhibition and induction interactions. Drug Metab Pharmacokinet. 25:28–47.

Giessmann T, May K, Modess C, Wegner D, Hecker U, Zschiesche M, Dazert P, Grube M, Schroeder E, Warzok R, Cascorbi I, Kroemer HK, Siegmund W (2004) Carbamazepine regulates intestinal P-glycoprotein and multidrug resistance protein MRP2 and influences disposition of talinolol in humans. Clin. Pharmacol. Ther. 76, 192–200.

Glaeser H, Drescher S, Eichelbaum M, Fromm MF (2005). Influence of rifampicin on the expression and function of human intestinal cytochrome P450 enzymes. Br J Clin Pharmacol.59(2):199-206.

Gorski JC, Vannaprasaht S, Hamman MA et al (2003) The effect of age, sex and rifampin administration on intestinal and hepatic cytochrome P450 3A activity. Clin Pharmacol. Ther. 74:275-287. PMID: 12966371.

Greiner B, Eichelbaum M, Fritz P, Kreichgauer HP, von Richter O, Zundler J, Kroemer HK (1999). The role of intestinal P-glycoprotein in the interaction of digoxin and rifampin. J Clin Invest 104: 147–53.

GTEx Consortium. The Genotype-Tissue Expression (GTEx) project. Nat. Genet. 45, 580–5 (2013).

Gupta A, Mugundu GM, Desai PB, Thummel KE, Unadkat JD (2008) Intestinal human colon adenocarcinoma cell line LS180 is an excellent model to study pregnane X receptor, but not constitutive androstane receptor, mediated CYP3A4 and multidrug resistance transporter 1 induction: studies with anti-human immunodeficiency virus protease inhibitors Drug Metab. Dispos., 36, 1172-1180.

Hartley DP, Dai X, Yabut J, Chu X, Cheng O, Zhang T, He YD, Roberts C, Ulrich R, Evers R, Evans DC (2006) Identification of potential pharmacological and toxicological targets differentiating structural analogs by a combination of transcriptional profiling and promoter analysis in LS-180 and Caco-2 adenocarcinoma cell lines. Pharmacogenet. Genomics, 16, 579–599.

Kararli TT (1995) Comparison of the gastrointestinal anatomy, physiology, and biochemistry of humans and commonly used laboratory animals. Biopharm. Drug Dispos. 16:351–80

Kasendra M, Luc R, Yin J, Manatakis DV, Kulkarni G, Lucchesi C, Sliz J, Apostolou A, Sunuwar L, Obrigewitch J, Jang K-J, Hamilton GA, Donowitz M, Karalis K (2020) Duodenum Intestine-Chip for Preclinical Drug Assessment in a Human Relevant Model. eLife, 9: e50135.

Larsen UL, Olesen HL, Nyvold GC, J. Eriksen J, Jakobsen P, Østergaard M, Autrup H, Andersen V (2007) Human intestinal P-glycoprotein activity estimated by the model substrate digoxin, Scandinavian Journal of Clinical and Laboratory Investigation, 67:2, 123-134.

Li AP, Alam N, Amaral K, Ho MD, Loretz C, Mitchell W, and Yang Q (2018) Cryopreserved human intestinal mucosal epithelium: a novel in vitro experimental system for the evaluation of enteric drug metabolism, P450 induction, and enterotoxicity. Drug Metab Dispos 46:1562–1571.

Madden LR, Nguyen TV, Garcia-Mojica S, Shah V, Le AV, Peier A, Visconti R, Parker EM, Presnell SC, Nguyen DG, Retting KN (2018) Bioprinted 3D Primary Human Intestinal Tissues Model Aspects of Native Physiology and ADME/Tox Functions, iScience, 2:156-167.

Maglich JM, Parks DJ, Moore LB, Collins JL, Goodwin B, Billin AN, Stoltz CA, Kliewer SA, Lambert MH, Willson TM, et al. (2003) Identification of a novel human constitutive androstane receptor (CAR) agonist and its use in the identification of CAR target genes. J Biol Chem 278:17277–17283.

McKinnon RA, Burgess WM, Hall PM, Roberts-Thomson SJ, Gonzalez FJ, McManus ME (1995). Characterisation of CYP3A gene subfamily expression in human gastrointestinal tissues. Gut. 36:259-267.

Meyer zu Schwabedissen HE, Oswald S, Bresser C, Nassif A, Modess C, Desta Z, Ogburn ET, Marinova M, Lütjohann D, Spielhagen C, Nauck M, Kroemer HK, Siegmund W (2012) Compartment-Specific Gene Regulation of the CAR Inducer Efavirenz In Vivo. Clin Pharmacol Ther 92: 103-111.

Miyoshi H, Stappenbeck TS (2013). In vitro expansion and genetic modification of gastrointestinal stem cells in spheroid culture. Nat Protoc. 8:2471-2482.

Mouly S, Lown KS, Kornhauser D, Joseph JL, Fiske WD, Benedek IH, and Watkins PB (2002) Hepatic but not intestinal CYP3A4 displays dose-dependent induction by efavirenz in humans. Clin Pharmacol Ther 72:1–9.

Mouly S and Paine, MF (2003) P-glycoprotein increases from proximal to distal regions of human small intestine. Pharm. Res.20: 1595–1599.

Müller J, Keiser M, Drozdzik M, and Oswald S (2017) Expression, regulation and function of intestinal drug transporters: an update. Biol Chem 398:175–192

Novotna A, Dvorak Z (2014) Omeprazole and Lansoprazole Enantiomers Induce CYP3A4 in Human Hepatocytes and Cell Lines via Glucocorticoid Receptor and Pregnane X Receptor Axis. PLoS ONE 9: e105580.

Oda S, Kato Y, Hatakeyama M, Iwamura A, Fukami T, Kume T, Yokoi T, and Nakajima M (2017) Evaluation of expression and glycosylation status of UGT1A10 in Supersomes and intestinal epithelial cells with a novel specific UGT1A10 monoclonal antibody. Drug Metab Dispos 45:1027–1034.

Onozato D, Yamashita M, Nakanishi A, Akagawa T, Kida Y, Ogawa I, Tadahiro H, Takahiro I, Tamihide M (2018). Generation of intestinal organoids suitable for pharmacokinetic studies from human induced pluripotent stem cells. Drug Metab Dispos. 46, 1572-1580.

Paine MF, Hart HL, Ludington SS, Haining RL, Rettie AE, and Zeldin DC (2006) The human intestinal cytochrome P450 “pie” Drug Metab Dispos. 34:880–886.

Pascussi JM, Drocourt L, Fabre JM, Maurel P, Vilarem MJ (2000) Dexamethasone induces pregnane X receptor and retinoid X receptor-alpha expression in human hepatocytes: synergistic increase of CYP3A4 induction by pregnane X receptor activators. Mol Pharmacol. 58:361-72

Peters WH, Kock L, Nagengast FM, Kremers PG (1991): Biotransformation enzymes in human intestine: critical low levels in the colon? Gut. 32: 408-412.

Sato T, Stange DE, Ferrante M, Vries RG, Van Es JH, Van den Brink S, Van Houdt WJ, Pronk A, Van Gorp J, Siersema PD, Clevers H (2011). Long-term expansion of epithelial organoids from human colon, adenoma, adenocarcinoma, and Barrett's epithelium. Gastroenterology. 141:1762-72.

Sato T, Vries RG, Snippert HJ, van de Wetering M, Barker N, Stange DE, van Es JH, Abo A, Kujala P, Peters PJ, Clevers H (2009) Single Lgr5 stem cells build crypt-villus structures in vitro without a mesenchymal niche. Nature. 459:262-265.

Schmiedlin-Ren P, Thummel KE, Fisher JM, et al. (2001) Induction of CYP3A4 by 1 alpha,25-dihydroxyvitamin D3 is human cell line-specific and is unlikely to involve pregnane X receptor. Drug Metab Dispos 29: 1446–1453.

Schuetz EG, Beck WT, and Schuetz JD (1996) Modulators and substrates of P-glycoprotein and cytochrome P4503A coordinately up-regulate these proteins in human colon carcinoma cells. Mol Pharmacol 49: 311–318.

Soars MG, Petullo DM, Eckstein JA, Kasper SC, Wrighton SA. (2004) An assessment of UDP-glucuronosyltransferase induction using primary human hepatocytes. Drug Metab Dispos. 32:140-148.

Thelen K and Dressman JB (2009) Cytochrome P450-mediated metabolism in the human gut wall. J Pharm and Pharmacol, 61: 541-558.

Thummel KE, Brimer C, Yasuda K, Thottassery J, Senn T, Lin Y, Ishizuka H, Kharasch E, Schuetz J, and Schuetz E (2001) Transcriptional control of intestinal cytochrome P-4503A by 1α, 25-dihydroxy vitamin D3. Mol Pharmacol 60:1399-1406.

van de Kerkhof EG, de Graaf IAM, Ungell A-LB, and Groothuis GMM (2008) Induction of metabolism and transport in human intestine: validation of precision-cut slices as a tool to study induction of drug metabolism in human intestine in vitro. Drug Metab Dispos 36:604–613.

VanDussen KL, Marinshaw JM, Shaikh N, Miyoshi H, Moon C, Tarr PI, Ciorba MA, and Stappenbeck TS (2015) Development of an enhanced human gastrointestinal epithelial culture system to facilitate patient-based assays. Gut 64:911–920.

VanDussen KL, Sonnek NM, Stappenbeck TS (2019). L-WRN conditioned medium for gastrointestinal epithelial stem cell culture shows replicable batch-to-batch activity levels across multiple research teams. Stem Cell Res. 37:101430.

Varma MV, Obach RS, Rotter C, Miller HR, Chang G, Steyn SJ, El-Kattan A, and Troutman MD (2010) Physicochemical space for optimum oral bioavailability: contribution of human intestinal absorption and first-pass elimination. J Med Chem 53:1098-1108.

Zhang L, Zhang YD, Strong JM, Reynolds KS, Huang, S-M (2008) A regulatory viewpoint on transporter-based drug interactions, Xenobiotica, 38:709-724

Zhang QY, Dunbar D, Ostrowska A, Zeisloft S, Yang J, and Kaminsky LS (1999) Characterization of human small intestinal cytochromes P-450. Drug Metab Dispos 27:804–809.

Zheng XE, Wang Z, Liao MZ, Lin YS, Shuhart MC, Schuetz EG, and Thummel KE (2012) Human PXR-mediated induction of intestinal CYP3A4 attenuates 1α,25-dihydroxyvitamin D3 function in human colon adenocarcinoma LS180 cells. Biochem Pharmacol 84:391–401.

Zhang Y, Benet, LZ (2001) The gut as a barrier to drug absorption: combined role of cytochrome P450 3A and P-glycoprotein. Clin. Pharmacokinet. 40: 159−168.

Footnotes

All authors are employees of AbbVie and may own AbbVie stock. AbbVie sponsored and funded the study; contributed to the design; participated in the collection, analysis, and interpretation of data; and participated in writing, reviewing, and approval of the final publication.

Portions of this work were originally presented at the 12th International ISSX Meeting 28–31 July 2019 Portland, Oregon, USA, P93.

Genotype-Tissue Expression (GTEx) Project was supported by the Common Fund of the Office of the Director of the National Institutes of Health, and by NCI, NHGRI, NHLBI, NIDA, NIMH, and NINDS (https://commonfund.nih.gov/about). The data used for the analyses described in this manuscript were obtained from: the GTEx Portal on 11/14/20.

Reprint requests should be sent to David Stresser, AbbVie, Inc, 1 North Waukegan Road, North Chicago, IL 60064, USA; David.Stresser@abbvie.com.

DMD Fast Forward. Published on December 18, 2020 as DOI: 10.1124/dmd.120.000281
This article has not been copyedited and formatted. The final version may differ from this version.

Figure legends

Figure 1. Effect of incubation time and a single treatment of 100 µM rifampin on the induction of CYP3A4 mRNA in ileal organoids from a single donor (donor 1). Data are from a single experiment and represent the means ± range of two replicates, each consisting of an analysis of a two pooled organoid-containing matrigel plugs.

Figure 2. Effect of rifampin on fold-induction of CYP3A4 mRNA only (A) and CYP3A4 and other transcripts shown in the figure legend (B) in ileal organoids compared to DMSO solvent vehicle treatment. In panel A, grey circles represent data points obtained from RT-PCR analysis of organoid pooled from two matrigel plugs across 5 independent experiments conducted over a two year span in a single donor (donor 1); Blue circles represent one experiment conducted in a different donor (donor 2). In panel B, each data point represents RT-PCR analysis of organoid pooled from two matrigel plugs in a single experiment (CYP1A1 data was from a single experiment conducted independently). Panels C and D are identical as described in panels A and B, except data were generated in colon organoids and 4 experiments were conducted for the CYP3A4 data generated in panel C. Statistical significance was determine by unpaired t-test and analysis was performed with CYP3A4 and rifampin treatments (donor 1 only) for ileal (A) and colon (C) organoids. Marked values (*, $p < 0.05$; **, $p < 0.01$) indicate those treatments that were statistically different than the 0.01 µM rifampin treatment, which was a value at or close to 1 (Geometric mean, 1.20; 95% CI 0.8737-1.648 for ileal organoids; 1.32; 95% CI 0.6649-2.620). Fits to data in panels A and C were global and included data points from both donors.

Figure 3. Effect of various inducers on CYP3A4 mRNA induction in ileal (panel A) or colon (panel B) organoids. Concentration units are micromolar. Grey symbols represent data points obtained across 2 to 4 experiments in a single donor (donor 1); Blue symbols represent one experiment conducted in a different donor (donor 2). Horizontal bars represent the geometric means and vertical bars represent the 95% confidence interval.

DMD Fast Forward. Published on December 18, 2020 as DOI: 10.1124/dmd.120.000281
This article has not been copyedited and formatted. The final version may differ from this version.

Figure 4. Effect of various inducers on CYP1A1 mRNA fold-induction over DMSO solvent vehicle in ileal (panel A) or colon (panel B) organoids. Concentration units are micromolar. Grey symbols represent data points obtained across 2 to 4 experiments in a single donor (donor 1); Blue symbols represent one experiment conducted in a different donor (donor 2). Horizontal bars represent the geometric means and vertical bars represent the 95% confidence interval. Insets, same data presented on log base 10 scale. Marked comparisons (*, $p < 0.05$; **, $p < 0.01$) indicate those treatments within donor 1 that were statistically different than the 10 µM phenytoin treatment (ileal) or 10 µM rifampin treatment (colon), which are data sets with mean values closest to 1 within each tissue (Geometric mean, 0.9944; 95% CI 0.4593-2.153 for ileal organoids; 0.97; 95% CI 0.6416-1.467 for colon organoids).

Figure 5. Effect of various inducers on CYP2B6 mRNA induction in ileal (panel A) or colon (panel B) organoids. Concentration units are micromolar. Symbols represent data points obtained across 2 experiments in a single donor (donor 1). Horizontal bars represent the geometric means and vertical bars represent the 95% confidence interval. Using 0.01 µM as a control value (geomean 1.198; 95% CI 0.7939-1.807, ileal; 0.8546, 95% CI 0.4526-1.614, colon) no treatment reached statistical significance (lowest adjusted p-value was 0.1867 with 100 µM omeprazole, colon).

Figure 6. Nifedipine oxidase activity in ileal organoids (donor 1) incubated with 5 or 50 µM nifedipine for 1 or 6 hours after a 48h treatment with 100 µM rifampin or DMSO solvent vehicle only (panel A). ND, Not detected. Marked comparisons (**, $p < 0.01$) indicate statistical difference. Panel B shows CYP3A4 fold-induction observed in same organoids used for nifedipine oxidase activity experiments following incubation with nifedipine for the time indicated. In both panels, horizontal bars represent the geometric means of 4 replicates (each replicate consistent of a pool of two organoid plugs) and vertical bars represent the 95% confidence interval.

DMD Fast Forward. Published on December 18, 2020 as DOI: 10.1124/dmd.120.000281
This article has not been copyedited and formatted. The final version may differ from this version.

Figure 7. Effect of rifampin (panel A) or various test compounds (panel B) on organoid cell viability (Cell-titer GLO 3D). Bars represent the mean of two replicates; Error bars indicate the range of the two values.

Figure 8. PXR expression is higher in ileal and colon organoids compared to CAR expression. To determine whether PXR and CAR were expressed in ileal and colon organoids during the conditions used for assays, RNA was extracted and expression of 18S (housekeeping gene) NR1I2 (PXR) and NR1I3 (CAR) levels quantified by qPCR. Specifically RNA was extracted from ileal and colon organoids from donor 1 after 3 days of growth in WRN conditioned media (green squares, represent the day 3 expression at the beginning of the assay when the inducers would be added), after the organoid were subsequently grown in media + EGF for 2 days (blue triangles, represent the expression in control samples on day 5 at the end of the assay), and after a subsequent growth in media + EGF + rifampin (purple triangles, represent the expression on day 5 after rifampin treatment at the end of the assay). In all treatments, based on Ct values, expression of PXR is significantly higher than CAR in both ileal (panel A) and colon (panel B) organoids. PXR Ct values ranged from 28 and 34, while CAR Ct values were all over 35 and in some cases undetectable, indicating lower levels or absence of expression in the model. Each data point represents the data from 2 pooled wells of organoids at the indicated timepoint and data from two independent studies performed in duplicate (4 data points total) are shown on the graph.

Figure 9. RNA-sequencing analysis of PXR and CAR gene expression from tissues in > 180 cadavers (data obtained from the Genotype-Tissue Expression (GTEx) project database, https://gtexportal.org/home/) showing > 20-fold less CAR expression in terminal ileum and colon compared to PXR. On the other hand, CAR expression was >2.3-fold higher than PXR in liver tissue. Values represent the median from analysis of 187 (ileum), 226 (liver) and 406 (colon) donors. It should be noted that TPM value are not comparable between tissues, since the value depends on the total number of transcripts recovered from tissues.

DMD Fast Forward. Published on December 18, 2020 as DOI: 10.1124/dmd.120.000281
This article has not been copyedited and formatted. The final version may differ from this version.

DMD Fast Forward. Published on December 18, 2020 as DOI: 10.1124/dmd.120.000281
This article has not been copyedited and formatted. The final version may differ from this version.

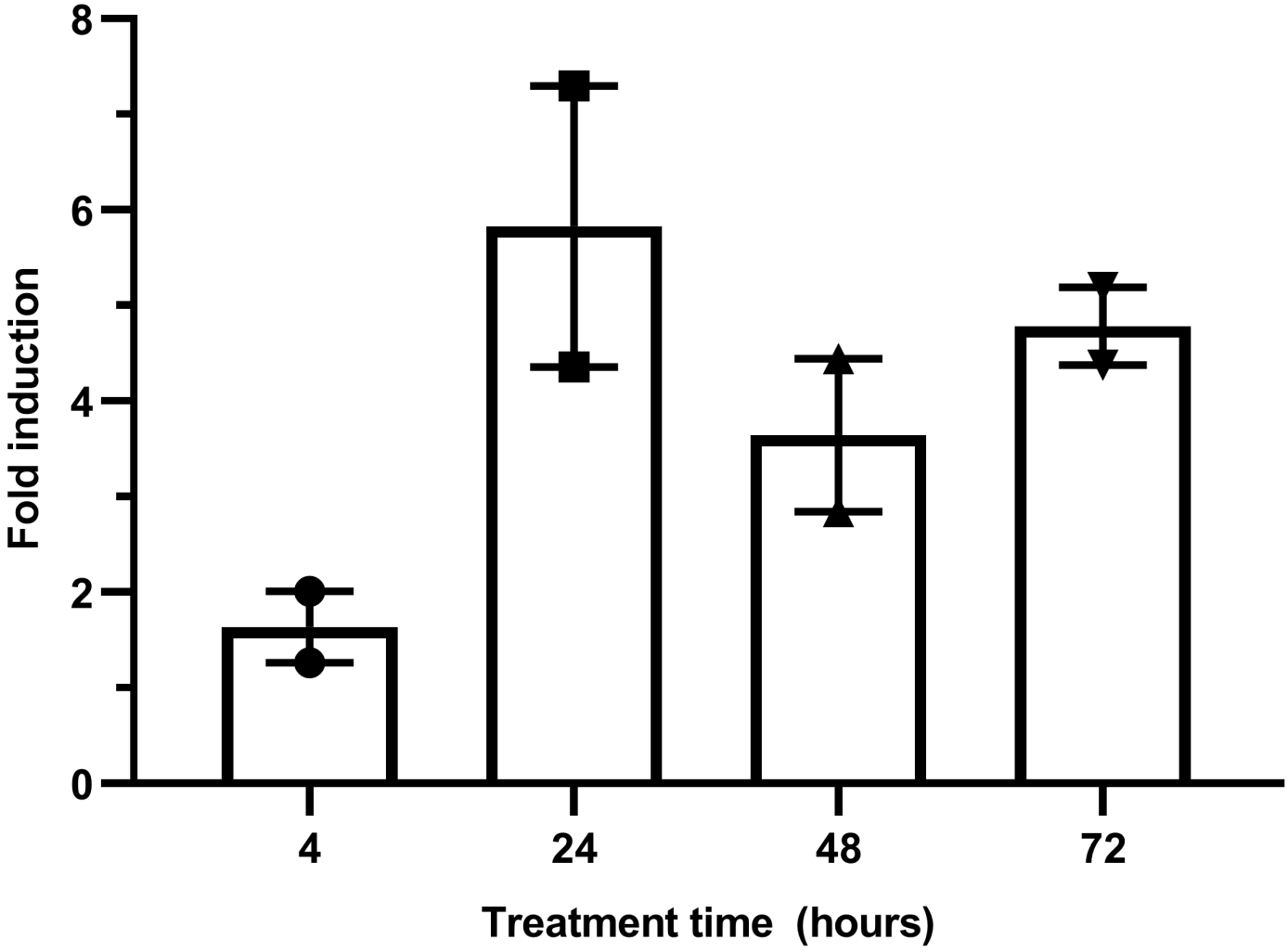

Figure 1

DMD Fast Forward. Published on December 18, 2020 as DOI: 10.1124/dmd.120.000281
This article has not been copyedited and formatted. The final version may differ from this version.

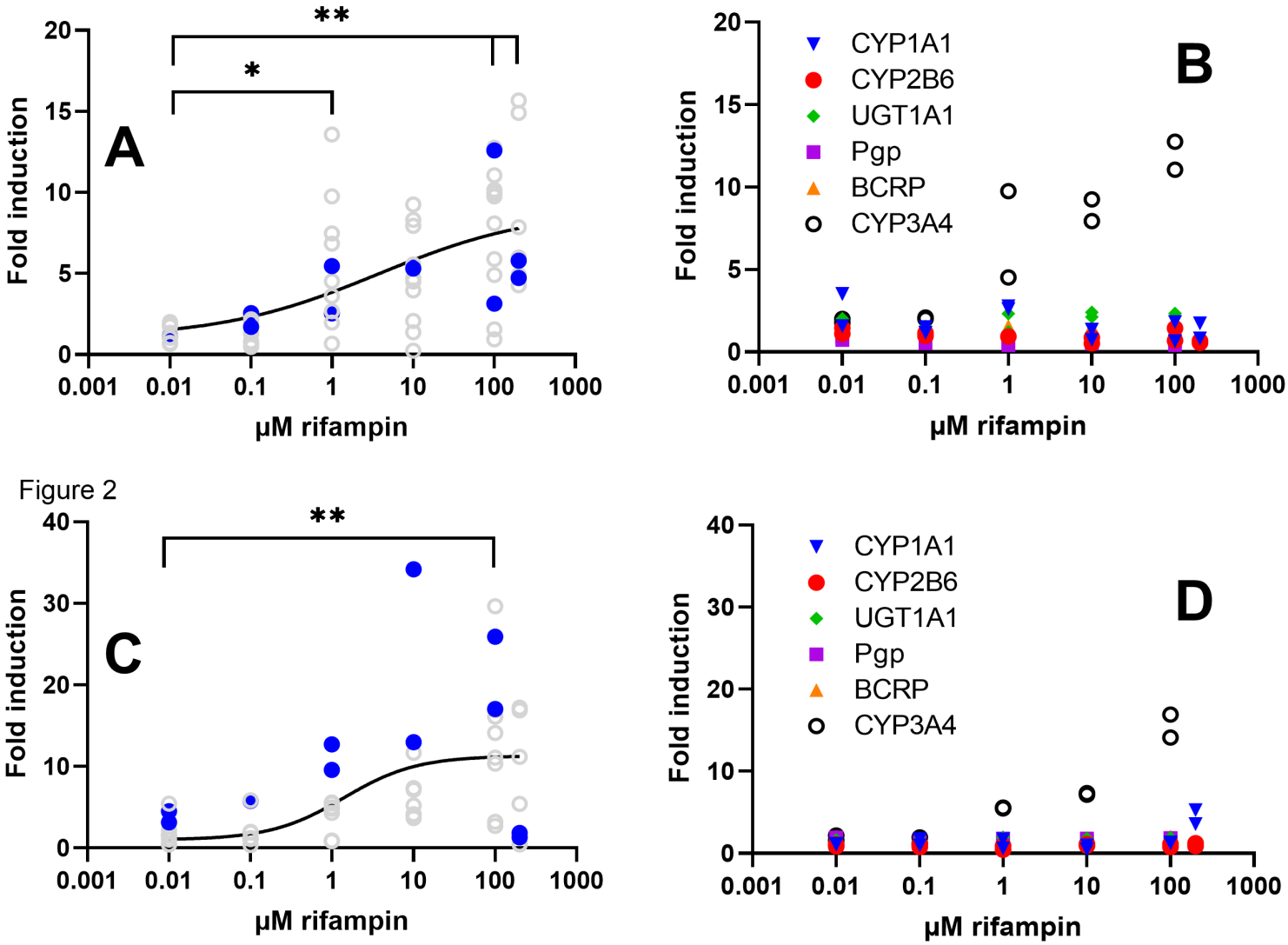

Figure 2

Figure 2

DMD Fast Forward. Published on December 18, 2020 as DOI: 10.1124/dmd.120.000281
This article has not been copyedited and formatted. The final version may differ from this version.

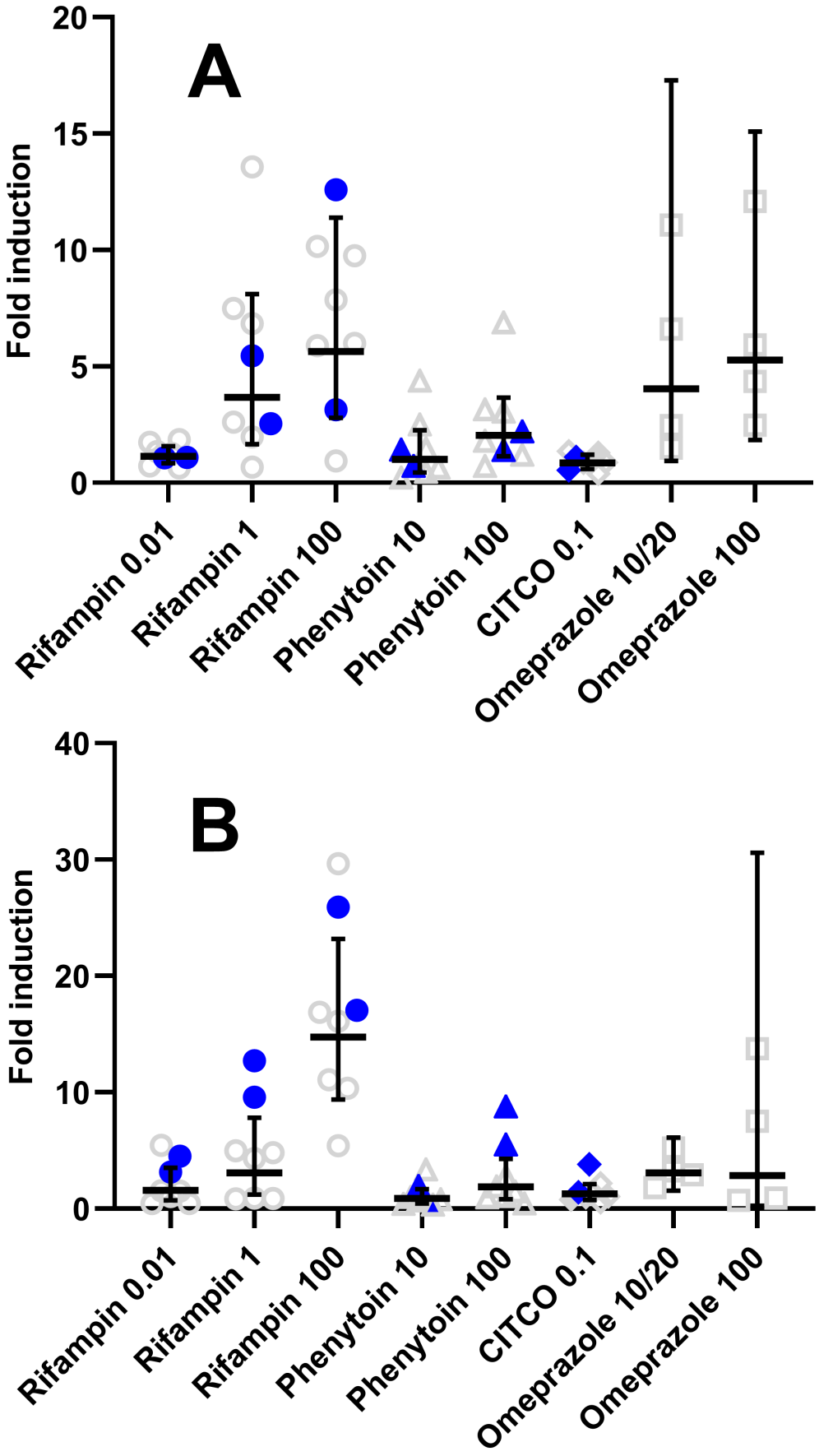

Figure 3

DMD Fast Forward. Published on December 18, 2020 as DOI: 10.1124/dmd.120.000281
This article has not been copyedited and formatted. The final version may differ from this version.

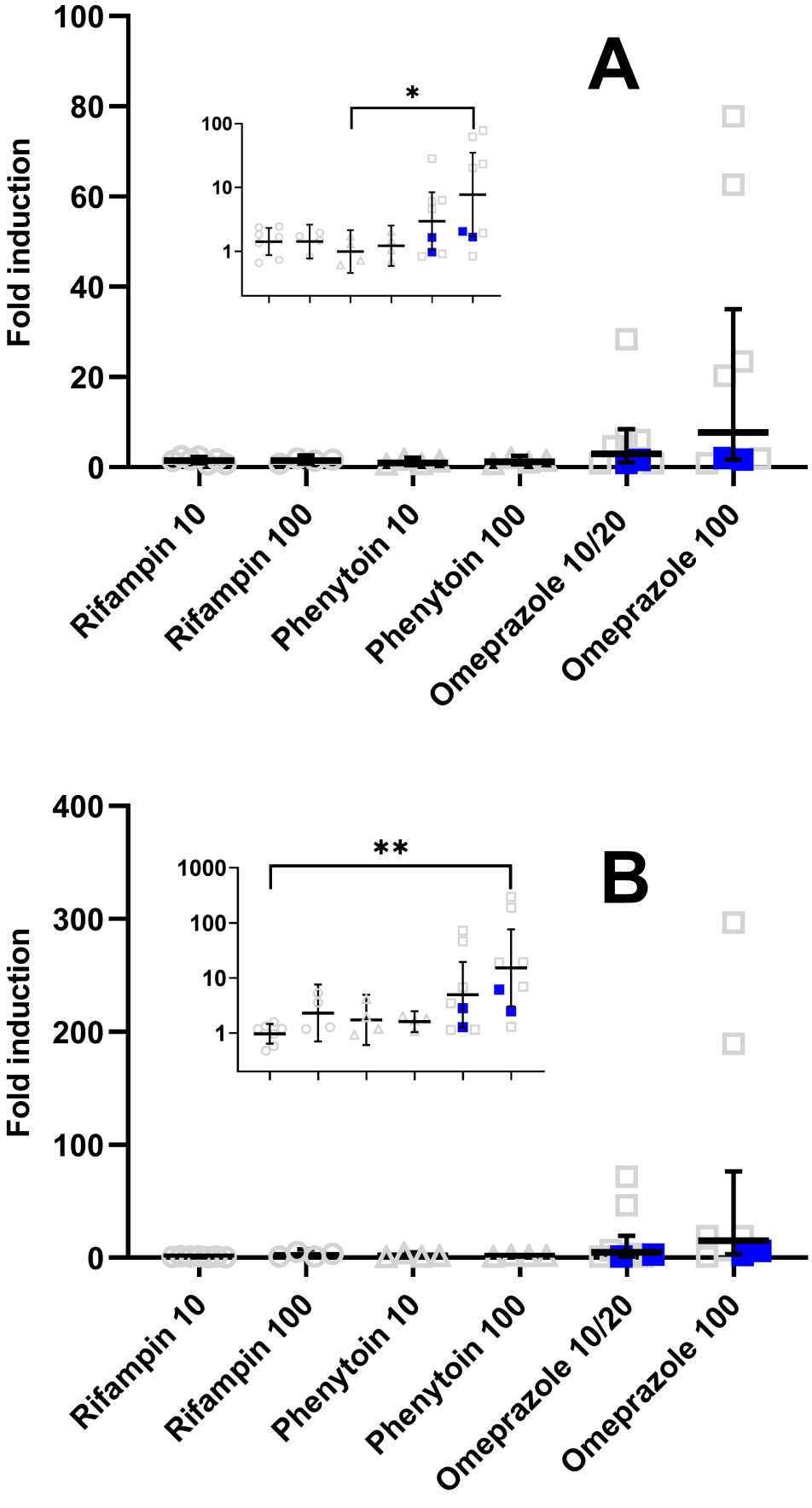

Figure 4

DMD Fast Forward. Published on December 18, 2020 as DOI: 10.1124/dmd.120.000281
This article has not been copyedited and formatted. The final version may differ from this version.

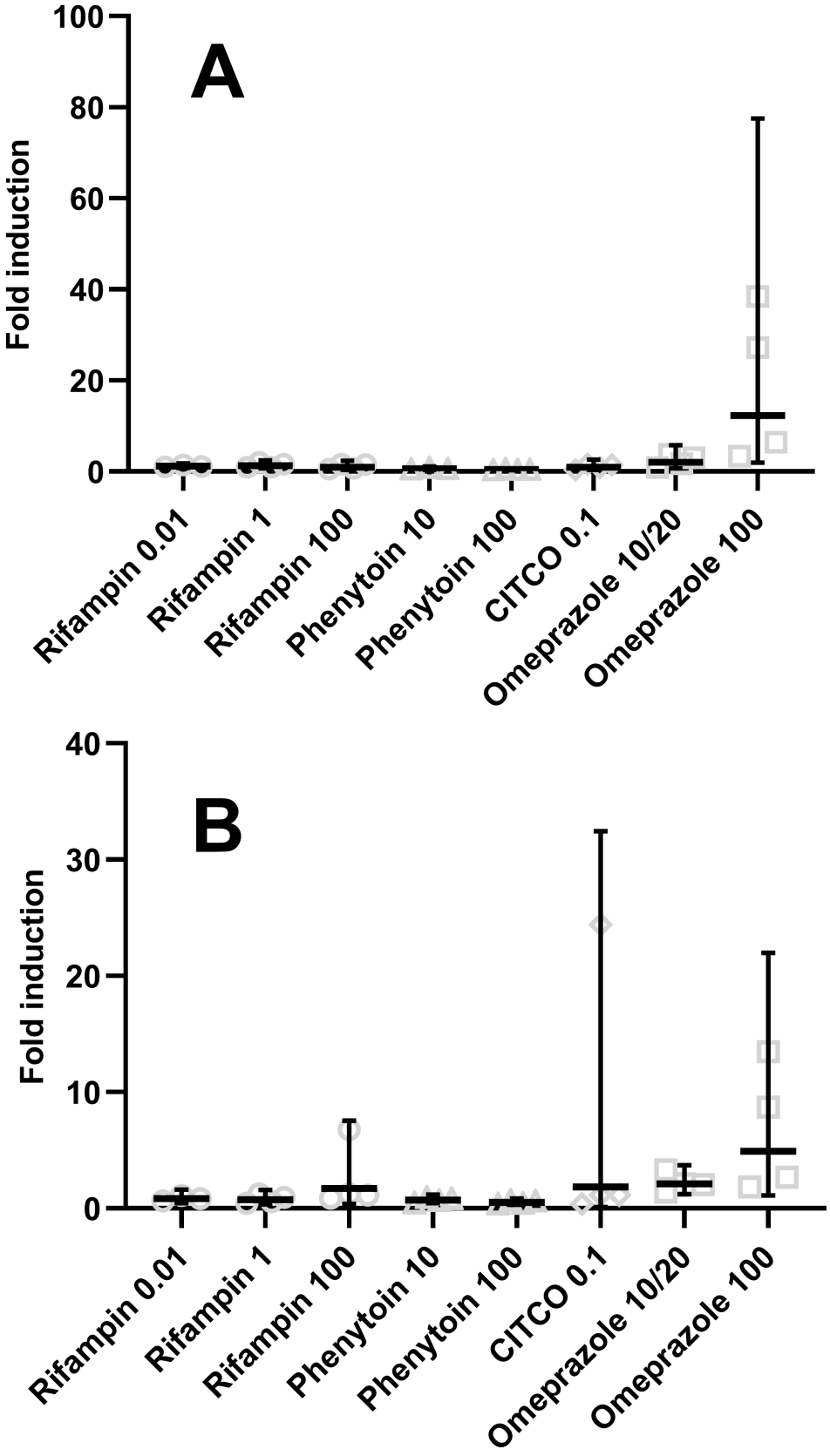

Figure 5

DMD Fast Forward. Published on December 18, 2020 as DOI: 10.1124/dmd.120.000281
This article has not been copyedited and formatted. The final version may differ from this version.

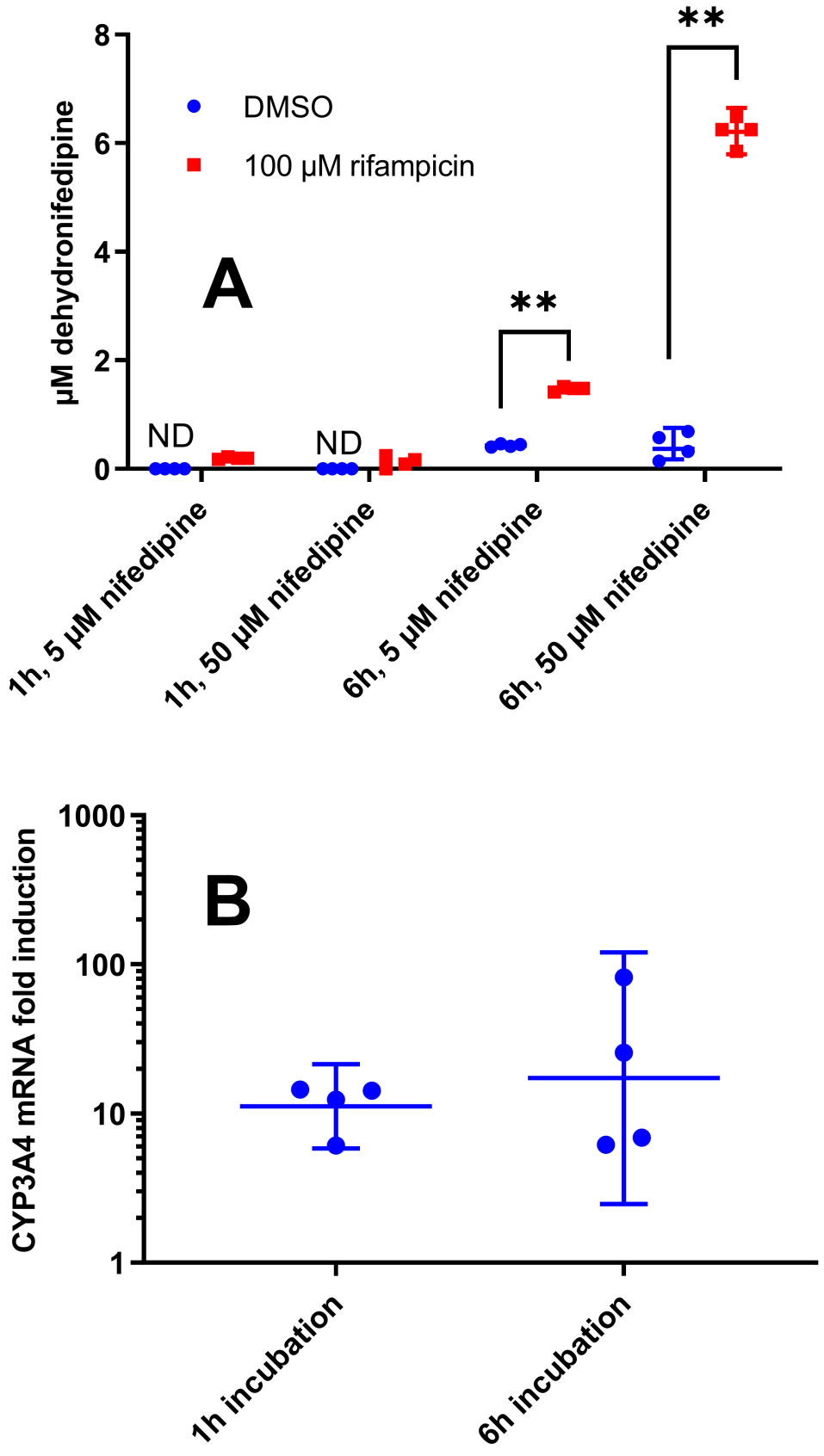

Figure 6

DMD Fast Forward. Published on December 18, 2020 as DOI: 10.1124/dmd.120.000281
This article has not been copyedited and formatted. The final version may differ from this version.

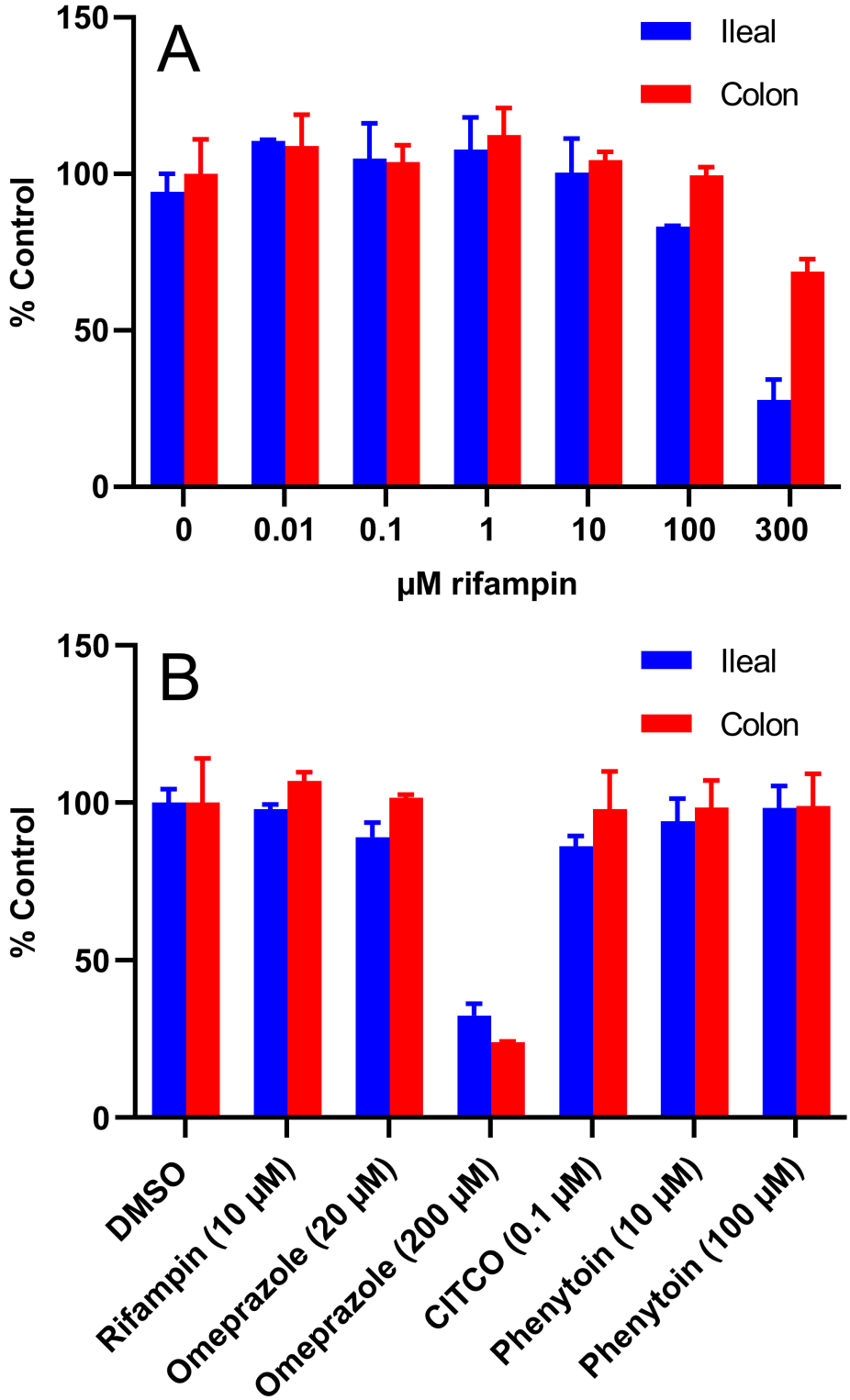

Figure 7

DMD Fast Forward. Published on December 18, 2020 as DOI: 10.1124/dmd.120.000281
This article has not been copyedited and formatted. The final version may differ from this version.

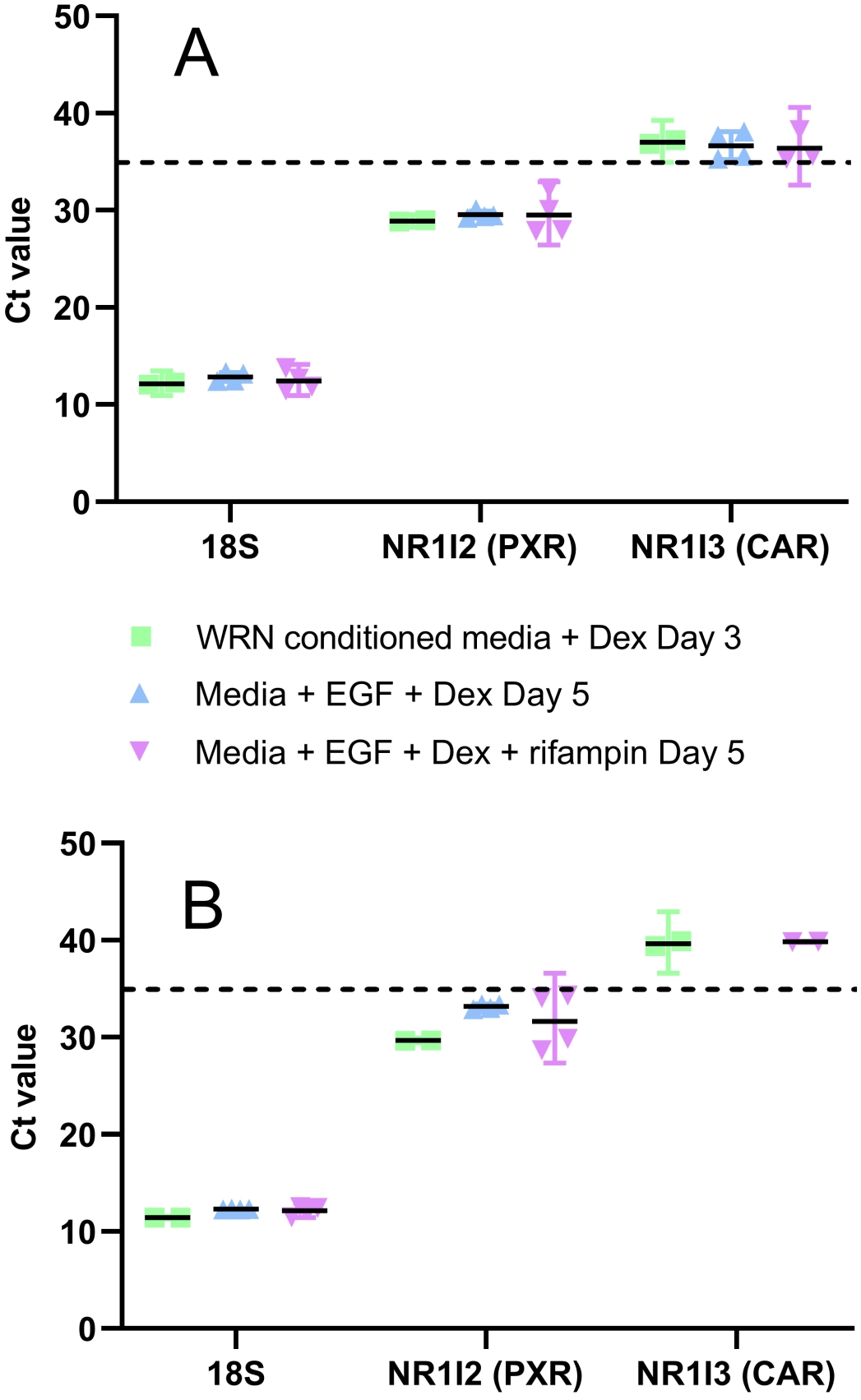

Figure 8

DMD Fast Forward. Published on December 18, 2020 as DOI: 10.1124/dmd.120.000281
This article has not been copyedited and formatted. The final version may differ from this version.

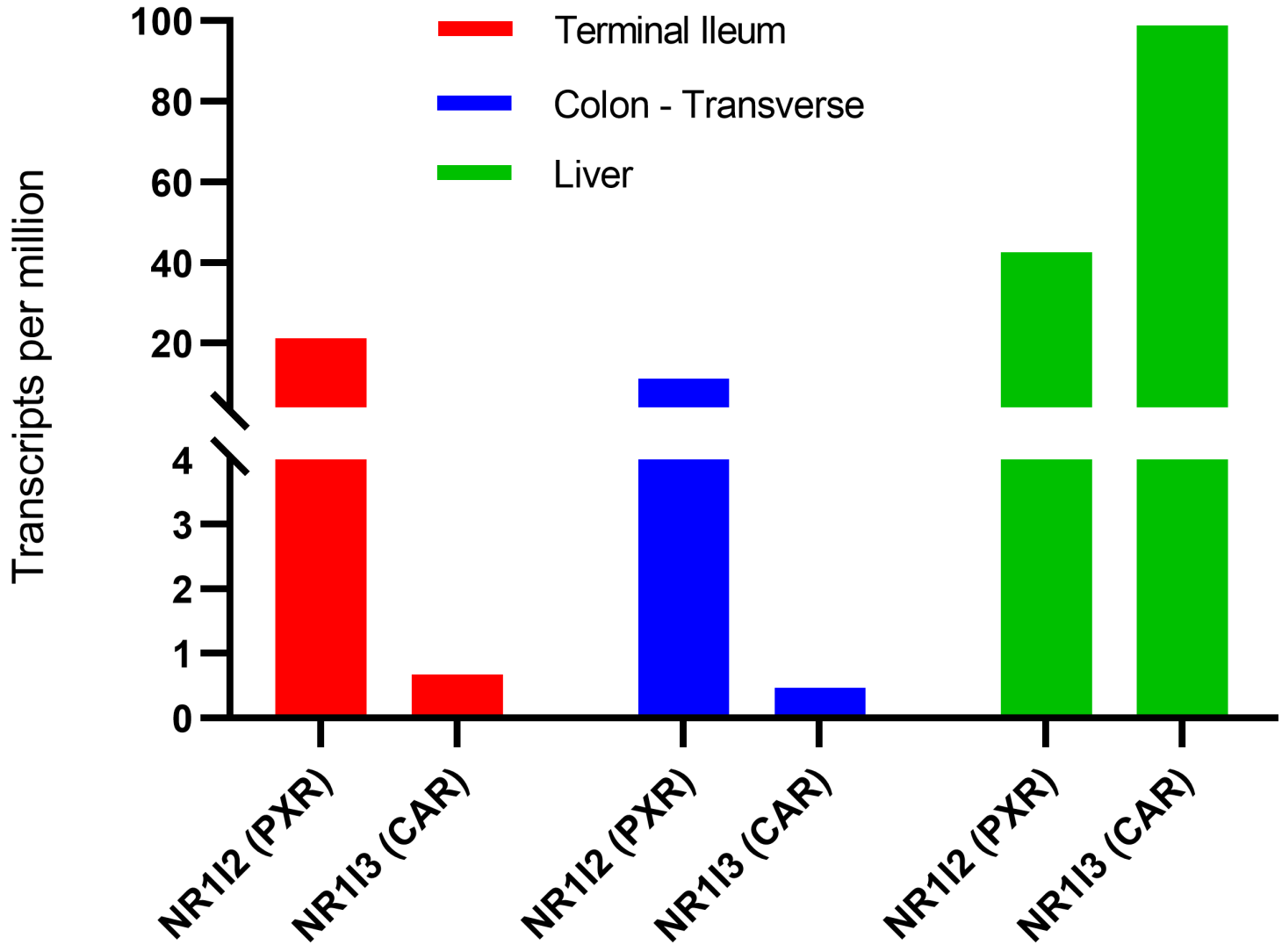

Figure 9